AIDA-2020-PUB-2018-001

AIDA-2020

Advanced European Infrastructures for Detectors at Accelerators

Journal Publication

Ultra High Fluence Radiation Monitoring Technology for the Future Circular Collider at CERN

Gorine, Georgi (CERN, EPFL) *et al*

26 January 2018

The AIDA-2020 Advanced European Infrastructures for Detectors at Accelerators project has received funding from the European Union's Horizon 2020 Research and Innovation programme under Grant Agreement no. 654168.

This work is part of AIDA-2020 Work Package **15: Upgrade of beam and irradiation test infrastructure**.

The electronic version of this AIDA-2020 Publication is available via the AIDA-2020 web site <http://aida2020.web.cern.ch> or on the CERN Document Server at the following URL: <http://cds.cern.ch/search?p=AIDA-2020-PUB-2018-001>

Ultra High Fluence Radiation Monitoring Technology for the Future Circular Collider at CERN

Georgi Gorine, *Student Member, IEEE*, Giuseppe Pezzullo, Igor Mandic, Anže Jazbec, Luka Snoj, Mar Capeans, Michael Moll, Didier Bouvet, Federico Ravotti, *Member, IEEE,* and Jean-Michel Sallese, *Member, IEEE*

***Abstract*— The Future Circular Collider (FCC) is foreseen as the next generation ~100 km long synchrotron to be built in the Geneva area starting 2050. This machine is expected to reach an energy level of 100 TeV generating unprecedented radiation levels >100 times higher than in today`s Large Hadron Collider (LHC). Current Radiation Monitoring system, like the RADMONs employed in the LHC, will not be capable to function and withstand this harsh environment. The development of a new Ultra High Fluence and Dose Radiation Sensor is a key element to allow irradiation tests of FCC equipment and, at a later stage, to monitor radiation levels in the FCC itself. In this paper, we present an innovative dosimetry solution based on thin layers of metals, which resistivity is shown to increase significantly due to the accumulated displacement damage. After describing the fabrication techniques used to manufacture these Radiation Dependent Resistors (RDR), we show and discuss the results of the irradiation experiments carried out with neutrons (up to 10^{18} n/cm^2 at the JSI TRIGA reactor) and with protons (up to $5.2\text{x}10^{16}$ p/cm^2 at CERN IRRAD facility) to validate the proposed concept of possible Ultra High Fluence FCC-dosimeter.**

***Index Terms* — Future Circular Collider, FCC, Radiation monitoring, Dosimetry, Radiation effects, Electrical characterization, Non-Ionizing Energy Loss, Displacement Damage, Radiation facilities, Neutron radiation effects, Proton radiation effects.**

I. Introduction

THE Future Circular Collider (FCC) is being designed to reach h-h collisions at an unprecedented collision energy levels of 100 TeV, about 8 times higher than in today`s Large Hadron Collider (LHC). Because of the increased energy and luminosity, during 10 years of FCC operation, radiation levels will likely reach tens of kGy (with $>10^{15}$ particles/cm^2) in certain sections of the FCC tunnel [1], and exceed several tens of MGy (with $>10^{17}$ particles/cm^2) inside the FCC experiments [2]. These estimations correspond to factors of 1000 (and 100) with respect to the expected conditions at LHC and High Luminosity LHC (HL-LHC), respectively [3]. To withstand such a harsh radiation environment special materials and technologies are required. This implies strict components selection and development of custom qualification protocols taking into account possible dependencies of the radiation response to different technologies [4].

A survey of state-of-the-art solid-state devices for radiation measurement showed that the current existing technologies are not capable of integrating such radiation levels, as well as of providing feasible solutions to build an on-line radiation monitor fulfilling the FCC requirements. For these reasons, a completely novel dosimetry technology is under development as potential solution for Ultra High Particle Fluence Monitoring. The proposed innovative solution consists of thin film metal structures, for which the resistivity varies according to the integrated particle fluence. The sensitivity to displacement damage, can then be trimmed by varying geometrical (thickness, width W, length L) and physical (material) properties of the thin-layers. The microfabrication of the devices was carried out at the Centre of Micronanotechnology (CMi) of the Ecole Polytechnique Fédérale de Lausanne (EPFL), and specific high-fluence irradiation tests, with high-energy neutrons and protons, have been performed in facilities at CERN, Geneva [5], and JSI, Ljubljana [6].

This paper is structured as follows: Section II gives an overview of the existing solid-state dosimeters as well as a description of the proposed dosimetry technology; Section III covers the Monte Carlo simulations covering the calculations of radiation damage on metals; Section IV describes the device fabrication and PCB production, as well as the different irradiation tests; Section V focuses on results of the irradiation tests; Section VI covers the discussion and Section VII gives our conclusions and outlines future work.

II. Dosimetry Technology

Current solid-state dosimeters employed at the High Energy Physics (HEP) experiments at the CERN LHC and in the accelerator tunnel itself, are based on the so-called RADMON devices (*PH-RADMON*, developed within the CERN Physics (PH) Department targeting the needs of LHC experiments [7] and *LHC-RADMON* for the tunnel areas [8]). These Radiation Monitoring systems are assembled with several specialized sensors, each capable of monitoring different type of radiation with different sensitivity and dynamic range [9]. As listed in Table I, RadFETs are used for measuring ionizing radiation by means of the increase of their threshold voltage due to charge trapping in the thick gate oxide. Selected p-i-n diodes are instead used for measuring fluence levels by correlating them

Paper submitted on September 29, 2017. This work was supported by the CERN Future Circular Collider, Special Technologies, Radiation Hardness Assurance, Work Package 11. This project has received funding also from the European Union`s Horizon 2020 research and innovation programme under grant agreement No 654168, with the AIDA-2020 Transnational Access project for the irradiation test at the JSI Triga Reactor in Ljubljana.

G. Gorine, G. Pezzullo, M. Moll, and F. Ravotti are with CERN, Geneva 23, CH-1211, Switzerland. (e-mail: Georgi.Gorine@cern.ch).

G.Gorine is also with École Polytechnique Fédérale de Lausanne, EPFL, Lausanne, CH-1015, Switzerland.

D. Bouvet and J. M. Sallèse are with École Polytechnique Fédérale de Lausanne, EPFL, Lausanne, CH-1015, Switzerland.

I. Mandic, A. Jazbec, and L. Snoj are with JSI, Jožef Stefan Institute, Jamova cesta 39, SI-1000, Ljubljana, Slovenia.

TABLE I
OPERATIONAL RANGE OF CURRENT PH-RADMON DEVICES FOR THE LHC EXPERIMENTS [7]

Device	Type	Energy Loss	Operating Range
LAAS	RadFET	Ionizing [Gy]	0.01 – 10
REM	RadFET	Ionizing [Gy]	10 – 100k
LBSD	p-i-n diode	Non Ionizing [n_{1MeV}/cm^2]	$1x10^8$ - $2x10^{12}$
BPW	p-i-n diode	Non Ionizing [n_{1MeV}/cm^2]	$2x10^{12}$ - $1x10^{15}$

TABLE II
MAX FLUENCE AND DOSE LEVELS AT CERN ACCELERATORS (AFTER 10 YEARS OF OPERATION) [1],[2]

Experiment	Luminosity [ab^{-1}]	Fluence[n_{1MeV}/cm^2]	Dose [MGy]
LHC	0.3	1.0×10^{15}	0.1
HL-LHC	3	1.5×10^{16}	4.8
FCC	3	2.8×10^{16}	9
FCC	30	2.8×10^{17}	90

with the increase of forward voltage due to displacement damage induced in the thick silicon base.

For both technologies, the key parameter is the thickness of the active layer which directly affects the sensitivity and the operational range of the dosimeter (RadFETs with gate oxide thickness between 0.13 µm and 1.6 µm , and p-i-n diodes with base thickness between 210 µm to 1000 µm [9]).

For the FCC, the maximum expected integrate, d dose and fluence, over 10 years of operation are shown in Table II. These values can be compared with the range covered by the *PH-RADMON* sensor in Table I. The noticeable limitation of the technology currently employed in the LHC, and the clear absence of any other adequate radiation monitoring device for fluence monitoring (as depicted in Figure 1), has pushed towards the research and development of a novel technology. At first, our focus has been on technologies for ultra-high fluence monitoring to upgrade the current *PH-RADMON* and cover the whole FCC operational range from $>10^{15}$ particles/cm^2 up to $3x10^{17}$ particles/cm^2. The innovative approach has been to exploit thin layers of metal instead of silicon, like in current NIEL (Non Ionizing Energy Loss) dosimeters [10]. Such choice was driven by the fact that submicrometer thin layers of metals are known to be less sensitive to low particle fluences (where silicon layers would be), but at the same time, sensitive to very high fluence, where structural and electrically observable effects occur. Such

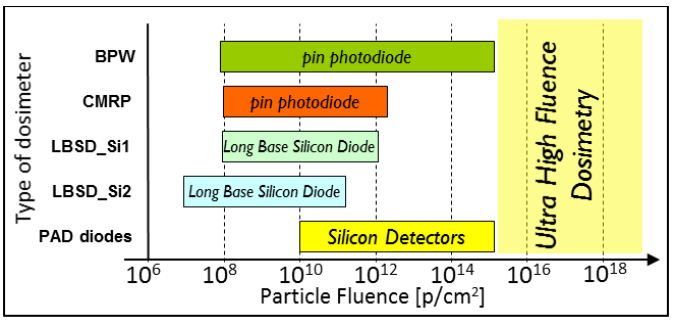

Fig. 1. Different solid-state NIEL dosimetry available on the market are shown with respect to their monitoring range. The highlighted and empty area in the Ultra High Fluence range indicates the target area of the technology presented in this paper.

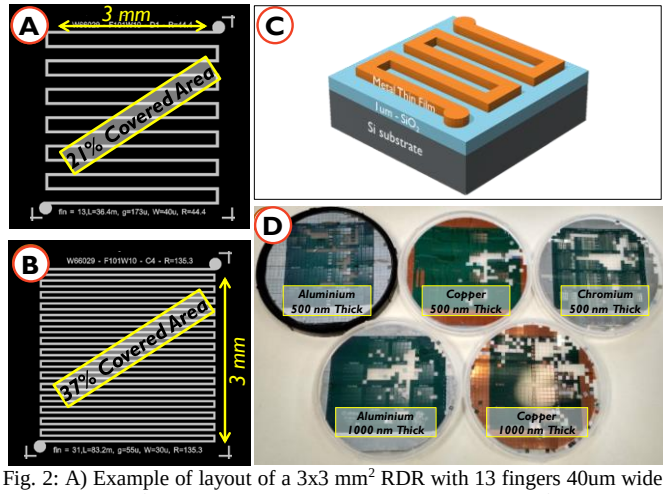

Fig. 2: A) Example of layout of a 3x3 mm^2 RDR with 13 fingers 40um wide covering 21% of the whole chip area, and B) an RDR with 31 fingers 30 um wide covering 37% of the area. A larger covered area may affect the overall device sensitivity. C) Schematic cross section of one RDR showing the stack Silicon Substrate/SiO_2/Metal. D) Picture of five produced wafers, with some of the chips removed for the electrical characterization.

property variations like changes in the material stiffness, generation of internal voids, surface swelling, and other, have been documented in literature [11]–[13]. In fact, displacement damage in metals is a known effect extensively studied in the past while developing materials and technologies for nuclear power plants [14] and space applications [15]. In the core of nuclear reactors, the particle flux can easily exceed 10^{15} n/cm^2/s, drastically increasing the probability of having atoms knocked from their initial positions in the crystal structures. This effect is usually expressed in units of DPA (Displacement Per Atom). The DPA accounts for how often atoms in an irradiated material are displaced due to an impinging particle (see Section III).

Several studies were made to correlate the number of vacancies and interstitials produced by the non-ionizing radiation with the change electrical resistivity of the material [16]–[18]. Similar resistivity measurements were also used for the characterization metals irradiated in reactors. The resulting experimental data have shown that the resistivity increase as function of particle fluence can be expressed by two specific components: one log-dependent, as result of the creation of defects in the lattice due to fast neutrons, and one linear as result of the transmutation mainly due to thermal neutrons [19].

Our proposed idea is therefore to profit of the resistivity variation in metals when exposed to high particle fluence, and to accomplish the FCC operational range and sensitivity requirements, by varying the dosimeter geometry (W, L, and thickness), using thin film technologies.

The proposed sensor shown in Figure 2, hereafter called Radiation Dependent Resistor (RDR), was made by sputtering thin layers of metal on silicon wafers and consecutive lithography and etching, into “serpentine shaped” resistive structures covering an area of 3x3 mm^2, as schematized in Figure 2.C. The selected materials for the produced RDRs were Aluminium, Chromium and Copper.

TABLE III
MATERIAL COMPOSITION OF THE RDRS AND SIMULATED DPA*

Material	Atomic Number	Lattice Structure	DPA Neutrons [DPA/(n/cm^2)]	DPA Protons [DPA/(p/cm^2)]
Aluminum (Al)	13	fcc	$3.21\text{x}10^{-20}$	$0.75\text{x}10^{-21}$
Chromium (Cr)	24	bcc	$1.91\text{x}10^{-20}$	$2.61\text{x}10^{-21}$
Copper (Cu)	27	fcc	$1.74\text{x}10^{-20}$	$3.85\text{x}10^{-21}$

**Simulations performed with FLUKA considering a target of 1x1x0.1 mm^3 with neutron energy spectrum of the TRIGA nuclear reactor* [34]*, and 23 GeV protons.*

TABLE IV
INITIAL RESISTANCE VALUES OF RDRS ON THE FOUR FCC-RADMON PCBS BEFORE IRRADIATION AT JSI AND IRRAD.

Material:	Al	Cr	Cu	Al	Cu
PCB1-JSI	621.9 Ω	1502.5 Ω	148.2 Ω	525.7 Ω	141.7 Ω
PCB2-JSI	211.0 Ω	906.4 Ω	67.9 Ω	242.9 Ω	55.4 Ω
PCB1-IRRAD	29.1 Ω	838.3 Ω	50.4 Ω	51.0 Ω	29.6 Ω
PCB2-IRRAD	49.2 Ω	1502.2 Ω	56.2 Ω	116.9 Ω	29.7 Ω

As shown in Table III, these three metals differ by their atomic number, as well as by their different crystallographic system (Body-Centered Cubic (bcc) Chromium and Face-Centered Cubic (fcc) Copper and Aluminium) [20]. Both characteristics have a strong impact on the defects production efficiency. The former because higher atomic number implies a greater amount of atoms thus increasing the interaction probability, the latter because fcc metals have a more compact lattice structure, consequently generating greater clusters, than the more open lattice of bcc metals [18]. More practically, the metals (Aluminium, Chromium, and Copper), were chosen also for their suitable properties for microfabrication, such as self-passivating, good adhesion with SiO_2 covered substrate, bondability (Al on Cr for wire-bonding pads), availability as targets for the sputtering machine, and also their relatively low level of induced radioactivity with respect to metals with even higher atomic number [21]. Table III also enlists the results obtained from radiation damage simulations, discussed in the following section.

III. SIMULATIONS DETAILS

Prior the realization of the first RDR prototypes, simulations were performed in order to assess the amount of displacement damage induced by extreme particle fluence in the different selected materials. Popular simulators used for calculating the radiation-matter interaction, such as SRIM [22], could not be used due to their intrinsic limitation to ions of energies below 2 GeV (high energy protons in IRRAD are at 23 GeV, see Section IV.D), but also due to a non-convergence in targets where the nuclear interaction length is much smaller than the target thickness. For these reasons, the FLUKA Monte Carlo tool [23], [24] has been used. The FLUKA scorecard used for the DPA calculation is *DPA-SCO* [25], and it accounts for every atom displaced from its initial location in the lattice, due to a primary or secondary impinging particle which recoil energy is higher than the lattice binding energy. For solving this calculation, FLUKA uses the theory of Norget, Robinson and Torrents [26], where both displacement efficiency and lattice displacement energy are taken into account. While the RDR sensors, as previously described, have a size of 3x3 mm^3 with a thickness of either 500 nm or 1000 nm, the target chosen for the simulation is of 1x1 mm^2 and 100 um thickness, to reach faster convergence. In the end, the DPA has been normalized per incoming particle (n^0 and p^+) per cm^2. Table III lists these simulation results in terms of total DPA integrated over the entire irradiation spectrum (for neutrons, the one of the central irradiation channel of the JSI TRIGA nuclear reactor, and for protons the one of the IRRAD proton facility. See sections IV.C and IV.D). From the simulated data, there was no straightforward conclusion on which material could offer better performance as dosimeter. For this reason, we decided to follow an empirical approach for this study, by producing and characterizing metal nanostructures with irradiation experiments.

IV. EXPERIMENTAL DETAILS

A. Devices Fabrication

The devices discussed in this work have been fully fabricated in the cleanroom facilities of EPFL Centre of Micronanotechnology (CMi) in Lausanne, Switzerland [27].

A total number of five 100 mm diameter wafers, were produced varying the metal type (Al, Cr, and Cu), and the metal thickness (500 nm and 1000 nm), as shown in Figure 2.C. Up to 300 devices were obtained on each wafer, but this number could be increased to 3000 by removing the test structures and covering the whole wafer area. The single die size was 3x3 mm^2 designed to be compatible with the hosting Printed Circuit Board (PCB) shown in Figure 3 and described in the next subsection IV.B. The chosen "serpentine shaped" layout of the chips shown in Figures 2.A and 2.B, allowed obtaining, in a limited area, resistance values ranging from few Ω to several kΩ by increasing the number of fingers (2 to 51) and by varying their width W (from 2 µm to 50 µm) while keeping a fixed length L of 3 mm. At the end of the fabrication process, the

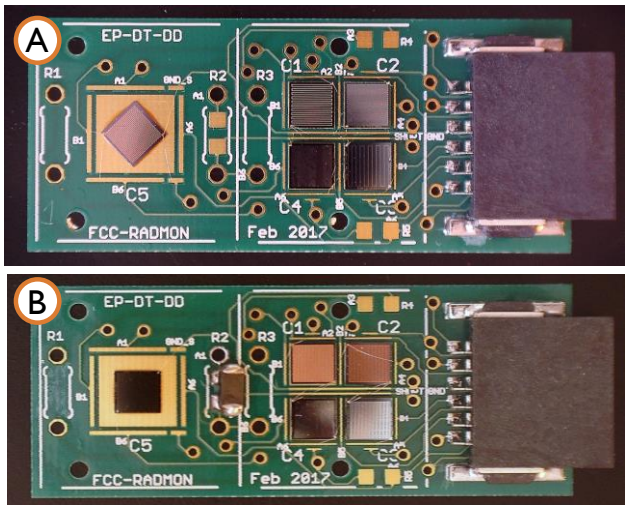

Fig. 3: Picture of two *FCC-RADMON* produced on a Doosan DS-7402 Hal-Free 0.2 mm substrate. A) PCB for the neutron irradiation with 5 wire-bonded RDRs, one for each wafer shown in Figure 2.C. B) PCB for the proton irradiation, also with 5 RDRs and an extra on-board NTC temperature sensor mounted in position R2.

wafers have been diced and a set of dies has been measured using a probe station at CERN. The selected dies have been wire-bonded (following a 4-wires readout schema) on the *FCC-RADMON* PCB to allow online measuring of the resistance variation while testing at different irradiation facilities.

B. Sensor Carrier for Ultra High Fluence Experiments

For compatibility reasons, the newly made PCB targeting FCC fluence levels, shown in Figure 3, follows the same layout of the Integrated Sensors Carrier [28] currently employed for the *PH-RADMON* installed in the LHC experiments (from which the name *FCC-RADMON* was chosen), and it mainly differs by the chosen substrate material. This upgrade over standard FR4 PCBs was needed after experiencing surface corrosion during another irradiation test with a high proton fluence exceeding $2x10^{16}$ p/cm^2 in the IRRAD Proton Facility. The new selected material is an halogen free and low phosphorus content substrate produced by Doosan (DS-7402) [29]. The *FCC-RADMON* PCB offers space for bonding up to four 3x3 mm^2 and one 5x5 mm^2 chips, along with several positions for discrete through-hole and SMD components (such as an on-board NTC temperature sensor). In the PCB configurations shown in Figure 3, five RDRs were mounted and wire bonded on each PCB following a 4-wire measurement schema (RDR initial values are listed in Table IV). The connection is then performed with a 12 channel IDC cable using the same ERNI connector as the current *PH-RADMON* system [7]. Until now, the produced PCBs have been successfully irradiated up to $1x10^{18}$ neutrons/cm^2 in a TRIGA nuclear reactor and $>5x10^{16}$ protons/cm^2 with a collimated 23 GeV proton beam, without showing any failures.

C. Neutron Irradiation at Jožef Stefan Institute

The produced RDRs were firstly tested in a neutron irradiation experiment at the TRIGA MARK II Nuclear Reactor of the Jožef Stefan Institute (JSI) in Ljubljana [30]. In about 40 hours, over 5 days of irradiation, a total neutron fluence of $1x10^{18}$ n/cm^2 has been reached in the central channel of the reactor, operated at a power of 250 kW. A picture of the reactor pool is shown in Figure 4.A. The broad neutron spectrum of the reactor is well characterized and stable during operation [6]. The following values have been used as reference flux for the central channel at 250 kW: $7.2x10^{12}$ n/cm^2/s calibrated using standard silicon diode dosimeters before starting our irradiation.

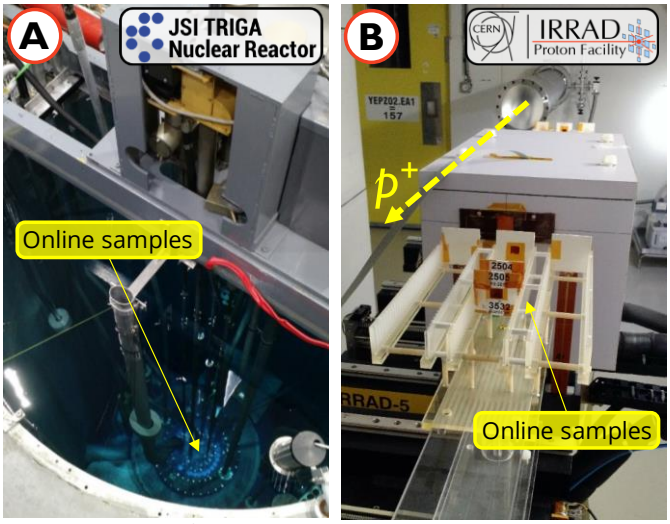

Fig. 4: A) Top view of the 5m deep JSI TRIGA reactor pool. The two FCC-RADMON boards were irradiated in the central channel (CC) pointed by the arrow. B) Photo of the Zone 1 inside the CERN IRRAD Proton Facility. The two FCC-RADMON boards were mounted on cardboard holders and positioned on the IRRAD7 motorized table, here ready to be inserted in *beam* position.

Two *FCC-RADMON* boards, like the one in Figure 3.A, taped with Kapton back-to-back, were inserted in a standard Aluminium cylindrical sample-holder to ensure mechanical protection during the insertion in the irradiation channel. Using two 12 channel IDC cables, the RDRs were connected to a test-bench located on the platform of the reactor, allowing an active readout of ten RDRs during the whole irradiation period (although a failure of the cable in the final stage of the irradiation limited the sampled data up to $9.4x10^{17}$ n/cm^2). These resistance measurements have been performed using a dedicated LabVIEW test-bench controlling an Agilent 34970A equipped with a 34901A switch matrix and a Keithley 2410 Source and Measure Unit (SMU). The switch matrix allowed to address each of the RDR under test and to connect them to the SMU for the 4-wires measurement to take place.

D. Proton Irradiation at CERN-IRRAD

Starting from June 2017, two similar *FCC-RADMONs* mounting the same set of previously described RDRs and an extra NTC temperature probe (Figure 3.B), are being irradiated at the CERN Proton Irradiation facility IRRAD [5]. As for the previously mentioned irradiation experiment, also in this case a dedicated LabVIEW test-bench was installed to allow an online monitoring of the RDRs resistance variation. After preparing the *FCC-RADMONs* on a cardboard holder, they were installed inside the IRRAD Proton Facility, as shown in Figure 4.B.

The irradiation is performed with a Gaussian (σ ~10 mm) pulsed 23 GeV proton beam extracted from the Proton Synchrotron (PS) accelerator. Each spill, sent every 10 seconds, has a typical duration of 400 ms and contains on average ~$5x10^{11}$ p/spill. Such flux allows reaching the HL-LHC required maximum fluence of $1.5x10^{16}$ n/cm^2 in less than two weeks, while it takes about an entire year (~10 months) of continuous irradiation to reach the final FCC fluence of $2.8x10^{17}$ n/cm^2.

The dosimetry over such long irradiation experiment is performed by interposing pure Aluminium foils in front of the *FCC-RADMONs* under irradiation (as shown in Figure 4.B) and replacing them every two weeks. Afterwards, a gamma spectrometry of the irradiated foil allows to estimate the proton fluence by counting the ^{22}Na activity in the foil as result of spallation reactions induced by the 23 GeV proton beam [31].

Even though the irradiation experiment will continue till the end of the 2017 CERN accelerators run, the preliminary data collected during 3 months, between June 7th and September 7th 2017, is shown and discussed in this paper. In such period a total proton fluence of $5.2x10^{16}$ p/cm^2 was reached.

V. Irradiation Tests Results

A. *Neutron Irradiation at Jožef Stefan Institute*

The two *FCC-RADMONs* were inserted inside the central channel before turning ON the reactor and measurements of every dosimeter were taken every minute. In Figure 5, the change in resistance of all the measured RDRs is shown against the increasing total integrated neutron fluence. Only data points sampled when the reactor was ON are plotted.

All devices have shown a significant change with resistance values increased by 5% for the Chromium samples, and up to 30% for the Aluminium samples. However, such abrupt rise of resistance is not only induced by displacement damage, but mainly by the temperature variation in the irradiation channel. This correlation with temperature can clearly be seen in Figure 6, where the temperature variation of the reactor fuel (dotted line) sampled over 120 hours, has been compared with the signal from the measured RDRs. The intermittent sudden decreases (and increases) in resistance value perfectly correspond to the points when the reactor was being driven from full power to zero (and back). Unfortunately, in this experiment, the *FCC-RADMON* boards did not include a temperature sensor due to the limited number of available channels on the PCB (12 total channels: 10 used for V_{sense} and V_{force} of 5 RDRs and 2 channels for shared GND_{sense} and GND_{force}). For that reason, successive measurements were performed in the same channel using a PT100 sensor contained in a similar Aluminium cylinder. This test, performed during two hours of operation at full power, has shown an inner channel temperature rising from about 25 °C to >65 °C rapidly after reaching reactor criticality. Also a temperature drift of about 0.5 °C/hour (with reactor at full power) has been observed. Such temperature variations are clearly affecting the resistance value of all the RDRs, as visible in Figure 5 (negative spikes), and in Figure 6 (the square wave, corresponding to the overnight shutdowns of the reactor). While the damage was not permanent for the Aluminium and Chromium samples, where the overnight annealing lead to almost full recovery, the Copper RDRs (*Cu-0.5u* and *Cu-1.0u* of PCB1) have shown a very promising result. As observable in Figure 6, no loss in the monitored dosimetry quantity is occurring once the reactor restarts. This is further confirmed, by the overnight almost-flat plateau (longer segments between square waves), where no considerable annealing is occurring. In fact, the resistance value goes back to the value it was before the night stop, and continues then to grow with increasing fluence.

At the end of the irradiation week, the two Copper RDR devices have shown an overall increase of resistance of 16.5 % and 13.5 % with respect to their initial values. Such increase was substantially higher during the first hours of irradiation (up to $1x10^{17}$ n/cm^2), where the sensitivity of the two Copper RDRs of PCB1 was of ~7.7 Ω/Φ_n (1000 nm thick RDR) and ~5.6 Ω/Φ_n (500 nm thick RDR) with $\Phi_n = 10^{17}$ n/cm^2. However, close to the end of the irradiation (from $5x10^{17}$ n/cm^2 to $1x10^{18}$ n/cm^2) the resolution dropped for both to ~0.5 Ω/Φ_n. It is interesting to notice that the change in resistivity of the 500 nm thick and the 1000 nm thick samples are very similar, indicating no big impact of the thickness on the final device sensitivity. On the other hand, a dependence of the sensitivity on the geometry has been observed when comparing the two mentioned Copper RDRs of PCB1, with respect to the other two Copper RDRs on PCB2 (*Cu-0.5u* and *Cu-1.0u* of PCB2 in Figure 6). The firsts are longer RDRs (more fingers, 51 instead of 31), but narrower (10 um instead of 30 um). This suggests that a greater sensitivity can be achieved by increasing the overall area of exposed metal (see different area layouts in Figures 2.A and 2.B), thus increasing the probability of a hit by an incoming particle.

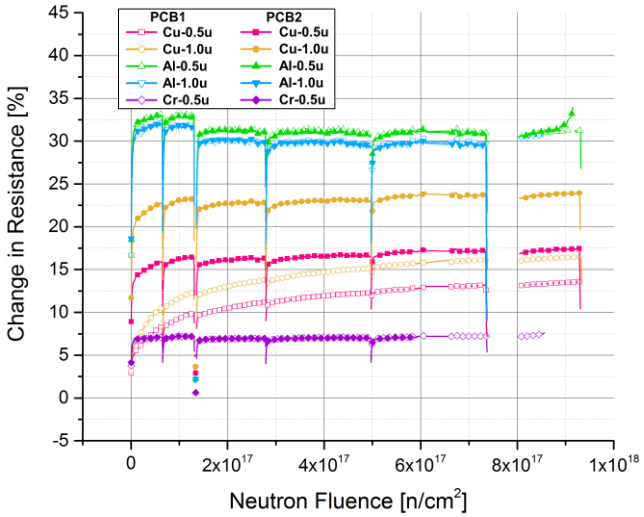

Fig. 5: Resistance variation from the initial value in % vs. the integrated neutron fluence, for each RDR with 0.5 um and 1.0 um thickness, on PCB1 and PCB2. The negative peaks correspond to the overnight ON-OFF-ON transitions of the reactor induced by abrupt changes in temperature. The void before $8x10^{17}$ n/cm^2 is due to data loss during acquisition while the interrupted curves towards the end of the irradiation are probably due to a failure of the cable at $9.4x10^{17}$ n/cm^2.

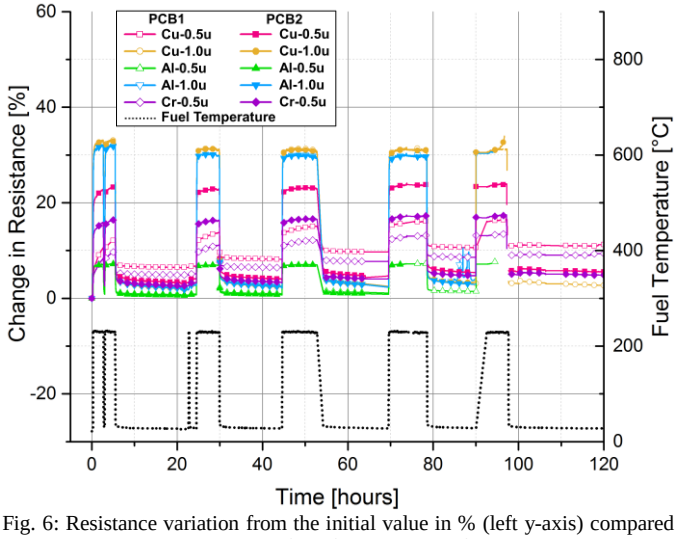

Fig. 6: Resistance variation from the initial value in % (left y-axis) compared with the temperature variations of the fuel elements of the reactor (black) over all the 5 days (120 h) of irradiation test (right y-axis). The points where the black curve is low at 25°C correspond to the overnight stops where the reactor was switched off, while all the RDRs either experienced annealing (like the Al and Cr samples) or stayed flat (like the Cu samples).

B. *Proton Irradiation at CERN-IRRAD*

As mentioned in Section IV.D, this irradiation experiment started in June 2017 and since then, it has continuously being irradiated, cumulating about $5x10^{15}$ p/cm^2 every week, reaching $5.2x10^{16}$ p/cm^2 in September 2017.

Since the beam spot is about 10 mm in diameter, only the four RDRs located next to the connector are being irradiated, while the fifth RDR (on both PCBs is the Chromium sample) is getting only the tails of the Gaussian distributed beam, thus negligible with respect to the total fluence collected by the other sensors. Not measuring the Cr samples allowed freeing channels for the readout of NTC temperature sensors (as shown in Figure 3.B). In addition, one of the sensors (*Al-0.5* of PCB1) experienced a failure after two months of irradiation at about $3.7x10^{16}$ p/cm^2. Therefore, only experimental data collected from the remaining seven sensors is discussed here. Figure 7 shows this data expressed in change of resistance of the RDRs with increasing proton fluence. From the graph it is clear that firstly, thanks to the stable temperature (21°C ±0.5°C), in the IRRAD bunker (NTC curves in Figure 7), no resistance variation can be attributed to temperature variations. Secondly, the impinging protons are inducing a noticeable damage successfully measurable in a variation of the resistance. Again the Copper samples are the ones most affected by the protons, and in particular the 1 um thick Copper RDR on PCB2 (*Cu-1u*) is showing the greater variation of almost 19 % with respect to its starting resistance, while the Aluminium samples stop at about 2.5 %. Overall, in the range between $1x10^{16}$ p/cm^2 and $5.2x10^{16}$ p/cm^2 the Copper RDR of PCB2 have shown an initial sensitivity of ~2.1 Ω/Φ_p reduced to ~0.68 Ω/Φ_p towards the end. The other Copper RDRs have all about the same constant slope of ~1.2 Ω/Φ_p. The remaining Aluminium RDRs stayed at 0 % for almost half irradiation time, after which they started raising with a sensitivity of about ~0.1 Ω/Φ_p, where $\Phi_p = 10^{16}$ p/cm^2 for all the previously expressed sensitivities.

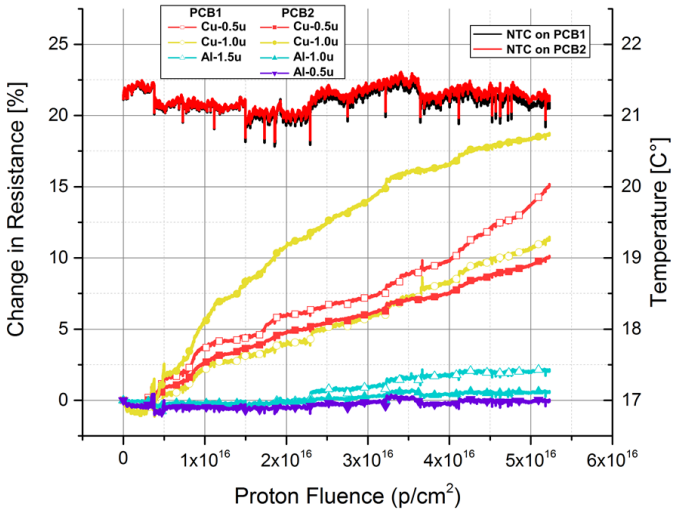

Fig. 7: Resistance variation from the initial value in % vs. the integrated proton fluence over 3 months of irradiation (left y-axis). The noisy peaks observable at ~$3.5x10^{16}$ p/cm^2, in the three PCB1 curves (pink, orange and yellow) are results of the correction introduced to compensate the failures of the fourth sensor Al-0.5u of PCB1 (not plotted). On the right y-axis, the on-board temperature as measured by the two NTC installed on each PCB.

As also stated before for the neutron irradiation experiment, the thickness of the RDR does not affect greatly the dosimeter performance. On the other hand, the greater sensitivity could be attributed to the larger number of fingers (31 instead of 13), but narrower (30 um instead of 40 um), once again suggesting that the top-geometry, as well as the amount of exposed metal, are the key factors controlling the dosimeter sensitivity. Differently from the logarithmic dependence of the neutron irradiated RDRs, in this case all RDRs follow a nearly linear law, apart from the *Cu-1u* of PCB2, which seems to approach saturation.

VI. Discussion

The two irradiation tests were planned to cumulate as much displacement damage as possible. In the case of the neutron irradiation, thanks to the very high flux, the targeted FCC-fluence has been reached and overtaken within 5 days. On the other hand, in the IRRAD proton facility, such high levels can be reached only after very long irradiation runs. While both irradiations qualify for testing material damage due to displacement, the very different particle type, energy spectrum and dose rate, do not allow for a straightforward comparison, and more irradiation data should be collected to find common scaling factors as it was done for silicon [32]. Furthermore, the very dissimilar irradiation conditions in terms of temperature, also introduce a fundamental point of divergence. In this context, the lack of temperature measurement on-board or of the irradiation channel during the neutron irradiation did not allow an appropriate data correction. Nevertheless, in the case of the Copper samples, and in some extent also the Aluminium RDRs, a clear constant increase is observable (in Figures 5 and 7) thus meaning that the high irradiation temperature and the daily night-stops did not always anneal completely the cumulated damage. Similarly in IRRAD, while no temperature problems have occurred, being kept stable (21°C ±0.5°C), both Copper (in much greater way) and Aluminium, have shown a measurable increase in resistance with increasing fluence.

Considering the simulated DPA values shown in Table III, in the case of the proton irradiation, the values are very consistent with the measured data, since Copper was correctly predicted to show about 5 times more DPA than for Aluminium, and thus, the hypothesis that DPA is directly proportional to the increase of resistivity is verified.

On the other hand, the simulations performed for the DPA generated during neutron irradiation, seem to not correlate with the measurements. This discrepancy could be due to the strong temperature dependence of the resistivity variation in the measured data and this will be furthered investigated during a second neutron irradiation next year.

VII. Conclusions and Future Work

An innovative dosimetry technology for Very High Fluence monitoring for the Future Circular Collider at CERN, has been discussed in this paper, describing its working principle based on radiation induced permanent change in resistivity of metal thin film called Radiation Dependent Resistors (RDR).

A special rad-hard *FCC-RADMON* PCB has been designed for hosting several RDRs made of Aluminium, Chromium and

Copper, of different sizes and with 1000 nm and 500 nm thickness, all entirely produced in cleanroom facilities.

Two irradiation tests have been performed: with neutrons, up to a total fluence of $1x10^{18}$ n/cm^2 at the MARK II TRIGA nuclear reactor of JSI in Ljubljana, and with 23 GeV protons, up to a total fluence of $5.2x10^{16}$ p/cm^2 at the IRRAD Proton Facility at CERN in Geneva.

The collected experimental data have shown a variation of resistivity with increasing particle fluence, confirming our concept of a dosimeter based on metal thin films. While no significant difference was found between the two chosen thin film thicknesses, the variation in the sensitivity to displacement damage can be attributed to different geometries (number of fingers and their width). Even greater impact was observed for different materials: Copper samples have shown the highest sensitivity for both irradiation tests, while Aluminium and Chromium samples exhibited a much weaker response.

Such material dependence has been confirmed by DPA simulations in the case of the proton irradiation, while for the neutron one, the excessive thermal annealing due to the >65°C temperature reached in the reactor during irradiation, have potentially altered the net DPA, thus not matching the resistivity measurement.

A deeper understanding of the effects of very high particle fluence on thin metal films and in particular the physical mechanisms that lead to an increase of the resistivity, will be the main focus of our future research.

As first, a larger amount of data will be available once the test in IRRAD will end in December 2017, cumulating a fluence of $1.2x10^{17}$ p/cm^2. In such way we will have a wider view of the RDRs behaviour over the whole FCC-range. Secondly another irradiation campaign will be performed in 2018 at the JSI TRIGA reactor, with *FCC-RADMONs* that have previously undergone a full electrical characterization in a climatic chamber, in order to extract the exact temperature coefficients of each device. This will allow to fully understand the effects of temperature on the metal structures, enabling to effectively disentangle the resistivity variation due to displacement from the one due to the temperature increase during irradiation.

In parallel, our research will focus on the basis of radiation damage on copper films, which have shown, in this study, the best performance as dosimeters. This will be done by testing a wider range of samples, fabricated with different deposition techniques (Physical Vapor Deposition (PVD), such as sputter and evaporator, and Atomic Layer Deposition (ALD)), different etching procedures (wet etching, ion beam etching, and lift-off) and with different thicknesses (5 nm and 50 nm). In particular, in collaboration with the University of Helsinki, we are going to study the effects of non-ionizing radiation on ALD Copper films of few nanometres [33] extending the experimental work presented in this paper for thicker films of 1000 nm and 500 nm, down to films of 5 nm.

ACKNOWLEDGMENTS

This work was supported by the CERN Future Circular Collider, Special Technologies Work Package 11, and has also received funding from the H2020 project AIDA-2020 Transnational Access, GA no. 654168.

The authors would like to thank Robert Froeschl (CERN-HSE/RP), Francesco Cerutti (CERN-EN/STI), and Klemen Ambrožič (JSI) for the DPA simulations. We would also like to express our gratitude to all the staff of the CMi cleanroom for their valuable support.

REFERENCES

[1] A. Infantino, R. G. Alía, M. I. Besana, M. Brugger, F. Cerutti, "Preliminary design of CERN Future Circular Collider tunnel: first evaluation of the radiation environment in critical areas for electronics," in *ICRS13*, 2016 [Online]. Available: doi.org/10.1051/epjconf/201715303004

[2] M. I. Besana, F. Cerutti, A. Ferrari, W. Riegler, V. Vlachoudis, "Evaluation of the radiation field in the future circular collider detector," *Phys. Rev. Accel. Beams*, vol. 19, no. 11, p. 111004, 2016 [Online]. Available: doi.org/10.1103/PhysRevAccelBeams.19.111004

[3] G. Apollinari, I. Béjar Alonso, O. Brüning, M. Lamont, L. Rossi, "High-Luminosity Large Hadron Collider (HL-LHC)," no. December, 2015 [Online]. Available: http://cds.cern.ch/record/2116337

[4] B. Camanzi, a G. Holmes-Siedle, "The race for new radiation monitors.," *Nat. Mater.*, vol. 7, no. 5, pp. 343–345, 2008 [Online]. Available: doi.org/10.1038/nmat2159

[5] B. Gkotse, M. Glaser, P. Lima, E. Matli, M. Moll, F. Ravotti, "A new high-intensity proton irradiation facility at the CERN PS east area," *Proc. Sci.*, pp. 1–5, 2014 [Online]. Available: pos.sissa.it/213/354

[6] L. Snoj, G. Žerovnik, A. Trkov, "Computational analysis of irradiation facilities at the JSI TRIGA reactor," *Appl. Radiat. Isot.*, vol. 70, no. 3, pp. 483–488, 2012 [Online]. Available: doi.org/10.1016/j.apradiso.2011.11.042

[7] F. Ravotti, M. Glaser, A. B. Rosenfeld, M. L. F. Lerch, A. G. Holmes-Siedle, G. Sarrabayrouse, "Radiation monitoring in mixed environments at CERN: From the IRRAD6 facility to the LHC experiments," *IEEE Trans. Nucl. Sci.*, vol. 54, no. 4, pp. 1170–1177, 2007 [Online]. Available: doi.org/10.1109/TNS.2007.892677

[8] G. Spiezia, J. Mekki, S. Batuca, M. Brugger, M. Calviani, A. Ferrari, D. Kramer, R. Losito, A. Masi, A. Nyul, P. Peronnard, C. Pignard, K. Roeed, T. Wijnands, "The LHC radiation monitoring system - RadMon," *Proc. Sci.*, pp. 1–12, 2011 [Online]. Available: http://pos.sissa.it/archive/conferences/143/024/RD11_024.pdf

[9] F. Ravotti, M. Glaser, "'SENSOR CATALOGUE' Data compilation of solid-state sensors for radiation monitoring," *Cern EDMS*, vol. TS-Note-20, 2005 [Online]. Available: https://edms.cern.ch/document/590497/1

[10] J. M. Swartz, M. O. Thurston, "Analysis of the effect of fast-neutron bombardment on the current-voltage characteristic of a conductivity-modulated p-i-n diode," *J. Appl. Phys.*, vol. 37, no. 2, pp. 745–755, 1966 [Online]. Available: doi.org/10.1063/1.1708249

[11] M. M. Ramsay, "The effect of neutron irradiation on thin film resistors," *Trans. Met. Soc. AIME*, vol. 239, pp. 917–919, 1967 [Online]. Available: doi.org/10.1016/0040-6090(68)90069-2

[12] J. Shewchun, W. R. Hardy, D. Kuenzig, C. Tam, "Reactively sputtered tantalum thin film resistors Part 2. Low energy, low fluence proton radiation damage," vol. 8, pp. 101–115, 1971 [Online]. Available: https://doi.org/10.1016/0040-6090(71)90002-2

[13] K. Farrel, A. E. Richt, "Microstructure and Tensile Properties of Heavily Irradiated 1100-0 Aluminum," in *Effects of Radiation on Structural Materials*, J. A. Sprague and D. Kramer, Eds. American Society for Testing and Materials, 1979, pp. 427–439 [Online]. Available: http://www.osti.gov/scitech/servlets/purl/6663374

[14] M. Kangilaski, "The effects of neutron radiation on structural materials," 1967 [Online]. Available: https://ntrs.nasa.gov/search.jsp?R=19680007407

[15] NASA, "Nuclear and space radiation effects on materials, NASA

Space Vehicle Design Criteria- (Structures)," no. June, 1970 [Online]. Available: https://ntrs.nasa.gov/archive/nasa/casi.ntrs.nasa.gov/19710015558.pdf

[16] J. W. Martin, "The electrical resistivity of some lattice defects in FCC metals observed in radiation damage experiments," *J. Phys. F*, vol. 2, no. 5, pp. 842-853, 1972 [Online]. Available: doi.org/10.1088/0305-4608/2/5/008

[17] S. J. Zinkle, "Electrical resistivity of small dislocation loops in irradiated copper," *J. Phys. F Met. Phys.*, vol. 18, no. 3, pp. 377-391, 1988 [Online]. Available: doi.org/10.1088/0305-4608/18/3/009

[18] M. Li, M. Eldrup, T. S. Byun, N. Hashimoto, L. L. Snead, S. J. Zinkle, "Low temperature neutron irradiation effects on microstructure and tensile properties of molybdenum," *J. Nucl. Mater.*, vol. 376, no. 1, pp. 11–28, 2008 [Online]. Available: doi.org/10.1016/j.jnucmat.2007.12.001

[19] R. L. Chaplin, R. R. Coltman, "Defects and transmutations in reactor-irradiated copper," *J. Nucl. Mater.*, vol. 108 & 109, pp. 175–182, 1982 [Online]. Available: doi.org/10.1016/0022-3115(82)90485-8

[20] R. B. Ross, *Metallic Materials Specification Handbook*, 4th ed. Boston, 1991 [Online]. Available: doi.org/10.1007 / 978-1-4615-3482-2

[21] F. Ravotti, R. Froeschl, "(CERN, Jan 2017, Private Communication)."

[22] J. F. Ziegler, M. D. Ziegler, J. P. Biersack, "SRIM – The Stopping and Range of Ions in Matter (2010)," *Nucl. Instr. Meth. B*, vol. 268, pp. 1818–1823, 2010 [Online]. Available: http://dtic.mil/dtic/tr/fulltext/u2/a515302.pdf

[23] A. Ferrari, P. R. Sala, A. Fasso, J. Ranft, "FLUKA: a multi-particle transport code," no. CERN-2005-10, 2005 [Online]. Available: doi.org/10.5170/CERN-2005-010

[24] T. T. Böhlen, F. Cerutti, M. P. W. Chin, A. Fassò, A. Ferrari, P. G. Ortega, A. Mairani, P. R. Sala, G. Smirnov, V. Vlachoudis, "The FLUKA Code: Developments and challenges for high energy and medical applications," *Nucl. Data Sheets*, vol. 120, pp. 211–214, 2014 [Online]. Available: doi.org/10.1016/j.nds.2014.07.049

[25] A. Fasso, A. Ferrari, G. Smirnov, F. Sommerer, V. Vlachoudis, "FLUKA Realistic Modeling of Radiation Induced Damage," *Prog. Nucl. Sci. Technol.*, vol. 2, pp. 769–775, 2011 [Online]. Available: http://inis.iaea.org/Search/search.aspx?orig_q=RN:43053566

[26] M. J. Norgett, M. T. Robinson, I. M. Torrens, "A proposed method of calculating displacement dose rates," *Nucl. Eng. Des.*, vol. 33, pp. 50–54, 1975 [Online]. Available: doi.org/10.1016/0029-5493(75)90035-7

[27] "CMI - Center of MicroNanoTechnology - EPFL" [Online]. Available: https://cmi.epfl.ch/

[28] F. Ravotti, M. Glaser, M. Moll, K. Idri, J. R. Vaillé, H. Prevost, L. Dusseau, "Conception of an integrated sensor for the radiation monitoring of the CMS experiment at the large hadron collider," *IEEE Trans. Nucl. Sci.*, vol. 51, no. 6 II, pp. 3642–3648, 2004 [Online]. Available: doi.org/10.1109/TNS.2004.839265

[29] "Doosan Electronics, Halogen-free Substrate Materials (DS-7402)" [Online]. Available: http://www.doosanelectronics.com/en/copper-clad-laminates-old/halogen-free-substrate-materials/fr-4-ds-7402/

[30] G. Žerovnik, T. Kaiba, V. Radulović, A. Jazbec, S. Rupnik, L. Barbot, D. Fourmentel, L. Snoj, "Validation of the neutron and gamma fields in the JSI TRIGA reactor using in-core fission and ionization chambers," *Appl. Radiat. Isot.*, vol. 96, pp. 27–35, 2015 [Online]. Available: doi.org/10.1016/j.apradiso.2014.10.026

[31] A. Curioni, R. Froeschl, M. Glaser, E. Iliopoulou, F. P. La Torre, F. Pozzi, F. Ravotti, M. Silari, "Single- and multi-foils $^{27}Al(p,3pn)^{24}Na$ activation technique for monitoring the intensity of high-energy beams," *Nucl. Instruments Methods Phys. Res. Sect. A Accel. Spectrometers, Detect. Assoc. Equip.*, vol. 858, no. November 2016, pp. 101–105, 2017 [Online]. Available: http://linkinghub.elsevier.com/retrieve/pii/S0168900217304199

[32] G. Lindstroem, M. Moll, E. Fretwurst, "Radiation hardness of silicon detectors - a challenge from high-energy physics," *Nucl. Instruments Methods Phys. Res. Sect. A Accel. Spectrometers, Detect. Assoc. Equip.*, vol. 426, no. 1, pp. 1–15, 1999 [Online]. Available: doi.org/10.1016/S0168-9002(98)01462-4

[33] K. Väyrynen, K. Mizohata, J. Räisänen, D. Peeters, A. Devi, M. Ritala, M. Leskelä, "Low-Temperature Atomic Layer Deposition of Low-Resistivity Copper Thin Films Using $Cu(dmap)_2$ and Tertiary Butyl Hydrazine," *Chem. Mater.*, vol. 29, no. 15, pp. 6502–6510, 2017 [Online]. Available: doi.org/10.1021/acs.chemmater.7b02098

[34] K. Ambrožič, G. Žerovnik, L. Snoj, "Computational analysis of the dose rates at JSI TRIGA reactor irradiation facilities," *Appl. Radiat. Isot.*, vol. 130, no. August, pp. 140–152, 2017 [Online]. Available: https://doi.org/10.1016/j.apradiso.2017.09.022